

# **Influence of tool rotational speed on microstructure and joint strength of friction stir spot welded pure copper**

I. Dinaharan<sup>a1\*</sup>, E. T. Akinlabi<sup>a2</sup>

<sup>a1\*</sup>Corresponding author–Post Doctoral Research Fellow, Department of Mechanical Engineering Science, University of Johannesburg, Auckland Park Kingsway Campus, Johannesburg 2006, South Africa. Email: dinaweld2009@gmail.com

<sup>a2</sup>Associate Professor, Department of Mechanical Engineering Science, University of Johannesburg, Auckland Park Kingsway Campus, Johannesburg 2006, South Africa. Email: etakinlabi@uj.ac.za

## **Abstract**

Copper is very difficult to be spot welded by conventional fusion welding techniques due to higher thermal diffusivity. Friction stir spot welding (FSSW) is a novel solid state welding process which is suitable and competent to spot weld copper. Commercially pure copper **sheets** of 3 mm thickness were spot welded by FSSW using industrial friction stir welding machine. The spot welds were made by varying the tool rotational speed at three levels. The spot welds were characterized using optical microscopy. The shear fracture load was evaluated using a computerized tensile testing machine. The results revealed that the tool rotational speed remarkably influenced the microstructure, shear fracture load and mode of fracture.

**Key words:** Copper, Friction Stir Spot welding, Microstructure, Shear Load.

## **1. Introduction**

Pure copper is extensively used in optical and electronic industries owing to its excellent properties such as good ductility, high electrical, thermal conductivity and good corrosion resistance. The welding of copper is often encountered in electrical, nuclear and

automobile industries [1,2]. Spot of welding of pure copper is generally hard to achieve by conventional fusion welding processes because of the high thermal diffusivity, which is about 10 to 100 times higher than in many steels and nickel alloys. The heat input required is much higher than in almost any other material. Further, pure copper is susceptible to solidification cracking and blowhole formation [3,4]. Friction stir spot welding (FSSW) is a novel solid state welding technique which is promising to spot weld copper without the problems associated with fusion welding techniques [5]

FSSW is a derivative process based on friction stir welding (FSW) which was developed at the welding institute in 1991. A number of differences exist between FSSW and FSW. One distinct difference is that there is no translation of tool during FSSW. FSW is commonly employed to join metallic plates in a butt configuration along a line of contact. On the other hand, FSSW is performed on smaller thickness plates kept in lap configuration. A rotating, non consumable, cylindrical shouldered tool with a pin is plunged at a predetermined feed rate into the overlapping plates to a depth slightly less than the total thickness of both the plates. Frictional heat is generated between the plate material and the rotating tool which plasticizes the material. The rotating action of the pin induces material flow in both the circumferential and axial directions. The axial force applied along the tool axis forges the plasticized material and forms an annular, solid state bond around the pin. At this moment, the rotating tool is retracted which leaves an exit hole. The major process parameters which influence the joint strength are Tool geometry, tool rotation speed, tool penetration depth, and dwell time. FSSW exhibits key advantages such as excellent mechanical properties, low distortion, ease of handling, low cost, and clean working environment [6–8].

FSSW technique has been successfully used to spot weld aluminum [9], magnesium [10], steel [11] and plastics [12]. Both similar and dissimilar spot welds were reported in

literatures [13,14]. FSSW of copper and its alloys are least explored. Barlas [15] spot welded pure copper and brass sheets using FSSW and analyzed the influence of tool rotational speed, dwell period and material location on microstructure and tensile shear fracture load (TSFL). He found that the weld parameters played an important role on the TSFL and failure mode. The TSFL increased with increase in the tool rotation speed and dwell time. Heideman [16] spot welded AA6061 and pure copper sheets and studied the effect of tool pin length, shoulder plunge depth, weld time and tool rotation speed on TSFL. Literatures on FSSW of pure copper are scanty. Therefore, the present work aims to spot weld copper sheets of 3 mm using FSSW and analyze the influence of tool rotational speed on the TSFL.

## 2. Materials and Methods

Commercially available pure copper sheets of 3 mm thickness were used in this study. The optical photomicrograph of as received copper sheet is shown in Fig. 1. Lap joint configuration was used to fabricate the spot welds where the rolling direction of material was kept parallel to the loading directions and the joint was initially obtained by securing the sheets in position using mechanical clamps. A non consumable tool made of high carbon steel was used to fabricate the joints. The tool had a shoulder of 18 mm and a conical profile of diameter varying from 5 mm to 3 mm along the length of pin. The pin length was 5.7 mm. An industrial purpose FSW machine (I-STIR) as depicted in Fig. 2 was used to FSSW. The FSSW procedure and welding cycle are depicted in Fig. 3. The tool rotational speed was varied in three levels of 1200 rpm, 1600 rpm and 2000 rpm. Other parameters were kept constant. The dwell period and axial force were 3 s and 10 kN respectively. Spot welds were made on two sheets clamped in lap configuration. Sufficient cooling was allowed between successive spot welds. The spot welded copper sheet is shown in Fig. 4. Six spot welds were made for each set of process parameters. Specimens were machined from the welded sheets

and polished semi automatically in a polishing machine (Struers LaboPol 25). The mirror polished specimens were etched with a color etchant containing 20 g chromic acid, 2 g sodium sulfate, 1.7 ml HCl (35%) in 100 ml distilled water. The macrostructure was recorded using a stereo microscope (OLYMPUS SZX16). The microstructure was observed using a metallurgical microscope (OLYMPUS BX51M). TSFL was evaluated using a computerized tensile tester (INSTRON 1195) at a crosshead speed of 2 mm/min.

### 3. Results and discussion

The macrographs of the friction stir spot welded copper as a function of tool rotational speed is presented in Fig. 5. It is possible to spot weld successfully using the chosen parameters. The weld zones are almost symmetrical with respect to the axis of keyhole. The tool rotation generates frictional heat which plasticizes the copper. The force applied along the axis of the tool promotes vertical motion of the plasticized copper. The axial force further consolidates the plasticized copper and a spot joint is formed. A clear joint width is visible in all the joints. A considerable area of both the top and bottom sheets is bonded together. The hook does not extend to the key hole area which means bonding existing between the sheets. The bond width was measured and was found to be 7.5 mm, 8.5 mm and 10 mm respectively at the selected tool rotation speeds. The increase in tool speed improved the bond width. Because the frictional heat generation is depended upon the tool rotational speed [17]. Higher the tool rotational speed higher will be the heat generation. Hence more copper is plasticized and the bond width increases.

Regions having different microstructures were observed on those macrographs. They are namely stir zone (SZ), thermomechanically affected zone (TMAZ), heat affected zone (HAZ) and base copper. These regions are presented in the micrographs in Fig. 6 as a function of tool rotational speed. The stir zone was adjacent to the key hole area and displays

very finer grains. FSSW was derived from FSW. The plasticized material in FSW undergoes dynamic recrystallization which results in the formation of fine grains. The width of stir zone reduces as tool rotational speed is increased due to higher heat input. TMAZ region presented slightly elongated grains with an array of oxide particles. The shearing of plasticized material from advancing side to retreading side causes the grains to elongate in this region. The width of TMAZ is found to reduce with an increase in tool rotational speed. The third region HAZ contained coarse grains in this region. The coarseness of the grains increased with an increase in tool rotational speed as presented in Fig. 7. The higher frictional heat generation causes the grains to coarsen. The grain size in HAZ region was higher compared to grain size of as received pure copper in Fig. 1. This region is clearly influenced by the frictional heat generation during FSSW which lead to grain growth. The stir zone was very thinner at higher tool rotational speed of 2000 rpm. The higher heat generation caused the recrystallized grains to grow further and diminished the width of stir zone. The microstructure of unbonded zone is presented in Fig. 8. The grains in upper and lower sheets are not uniform. The grains in the upper sheet are coarser than the lower sheet. This can be attributed to the proximity of each sheet to the tool shoulder. The upper sheet receives more heat input compared to the lower sheet which causes the grains to coarsen.

The influence of tool rotational speed on the TSFL is depicted in Fig. 9. It is evident from the figure that the increase in tool rotational speed increased TSFL. Although the increase in tool rotational speed caused grain growth in different regions across the joint, the TSL improved upon tool rotational speed. Because, the TSFL depends upon the joint width and the hook position from the stir zone area. A hook is formed in FSSW joints as material from the bottom sheet flow upwards during the process. The distance of the hook from the stir zone area determines the load carrying capacity of the joint. The hook is not clear in the

macro graph in Fig.1 due to annealing effect of copper during FSSW. The other factor is the bond width. The bond width increased with an increase in tool rotational speed. This provided more tangential area to resist the external load. Hence, TSFL increase as tool rotational speed was increased. The photographs of the failed specimens are shown in Fig. 10. The failed specimens demonstrate different mode of failures. The mode of failure is observed to be nugget pullout at tool rotational speed of 1200 rpm and 1600 rpm. It can be inferred from the photographs (Fig. 10a and b) that the nugget pull out originated from bottom of the key hole area. The diameter of the hole in the upper failed **sheet** is higher at 1500 rpm than 1200 rpm. This is due to an increase in bond width which provided wider metallurgical bonding. The mode of failure at tool rotational speed of 2000 rpm is tearing. The tearing started circumferentially around the unbonded region and could not pull the nugget out. Because the higher bond width at 2000 rpm caused the **sheet** to tear like a tensile specimen. The load versus displacement curve of tensile shear tested specimen at tool rotational speed of 1600 rpm is presented in Fig. 11. The load increases with constant slope until point 'c' is reached. The corresponding photographs of each point marked in Fig. 11 are detailed in Fig. 12. As the load is increased to point 'b' the specimen bends. The axis of the normal load does not coincide with the centre of the tested specimen which creates a small moment causing bending. The specimen starts yielding i.e. the nugget pull out commences at point 'c'. The load does not drop sharply to zero unlike tensile failures. Because the nugget pull out is not instant. The nugget gradually pulls out as separation increases until point 'g' is reached. The load drops to zero which indicates complete separation of both the **sheets**.

#### **4. Conclusions**

Commercially pure copper **sheets** were successfully spot welded using the novel technique FSSW. The influence of the key processing parameter tool rotational speed on

microstructure and TSFL was analyzed. The increase in tool rotational speed increased the bond width and coarsened the grains in stir zone and HAZ. TSFL improved as tool rotation is increased. The mode of failure was nugget pull out at 1200 rpm and 1600 rpm and tear out at 2000 rpm.

## References

- [1] K. Surekha, A. Els-Botes, *Materials and Design*, 32 (2011) 911–916, doi:10.1016/j.matdes.2010.08.028
- [2] P. Xue, B.L. Xiao, Q. Zhang, Z.Y. Ma, *Scripta Materialia*, 64 (2011) 1051–1054, doi:10.1016/j.scriptamat.2011.02.019
- [3] R. M. Leal, N. Sakharova, P. Vilaca, D. M. Rodrigues, A. Loureiro, *Science and Technology of Welding and Joining*, 16 (2011) 146–152, doi: <http://dx.doi.org/10.1179/1362171810Y.0000000005>
- [4] W. B. Lee, S. B. Jung, *Materials Letters*, 58 (2004) 1041– 1046, doi:10.1016/j.matlet.2003.08.014
- [5] M. I. Khan, M. L. Kuntz, P. Su, A. Gerlich, T. North, Y. Zhou, *Science and Technology of Welding and Joining*, 12 (2007) 175–182, doi: <http://dx.doi.org/10.1179/174329307X159801>
- [6] J. Jeon, S. Mironov, Y.S. Sato, H. Kokawa, S.H.C. Park, S. Hirano, *Acta Materialia*, 59 (2011) 7439–7449, doi:10.1016/j.actamat.2011.09.013
- [7] Y.F. Sun, H. Fujii, N. Takaki, Y. Okitsu, *Materials and Design*, 37 (2012) 384–392, doi:10.1016/j.matdes.2012.01.027
- [8] S. Bozzi, A. L. H. Etter, T. Baudin, B. Criqui, J.G. Kerbiguet, *Materials Science and Engineering A*, 527 (2010) 4505–4509, doi:10.1016/j.msea.2010.03.097

- [9] G. Buffa, L. Fratini, M. Piacentini, *Journal of Materials Processing Technology* 208 (2008) 309–317, doi:10.1016/j.jmatprotec.2008.01.001
- [10] Y.H. Yina, N. Sun, T.H. North, S.S. Hu, *Journal of Materials Processing Technology*, 210 (2010) 2062–2070, doi:10.1016/j.jmatprotec.2010.07.029
- [11] C. C. P. Mazzaferro, T. S. Rosendo, M. A. D. Tiera, J. A. E. Mazzaferro, J. F. Dos Santos, T. R. Strohaecker, *Materials and Manufacturing Processes*, 30 (2015) 1–14, doi:10.1080/10426914.2015.1004699
- [12] P. H. F. Oliveira, S. T. A. Filho, J. F. dos Santos, E. Hage, *Materials Letters*, 64 (2010) 2098–2101, doi:10.1016/j.matlet.2010.06.050
- [13] M. Yamamoto, A. Gerlich, T. H. North, K. Shinozaki, *Science and Technology of Welding and Joining*, 13 (2008) 583–592, doi:  
<http://dx.doi.org/10.1179/174329308X349520>
- [14] V. X. Tran, J. Pan, T. Pan, *International Journal of Fatigue*, 32 (2010) 1022–1041, doi:10.1016/j.ijfatigue.2009.11.009
- [15] Z. Barlas, *International Journal of Advanced Manufacturing Technology* 80 (2015) 161–170, doi: 10.1007/s00170-015-6998-1
- [16] R. Heideman, C. Johnson, S. Kou, *Science and Technology of Welding and Joining*, 15 (2010) 597–604, doi: <http://dx.doi.org/10.1179/136217110X12785889549985>
- [17] R. S. Mishra, Z. Y. Ma, *Materials Science and Engineering R*, 50 (2005) 1–78, doi:10.1016/j.mser.2005.07.001



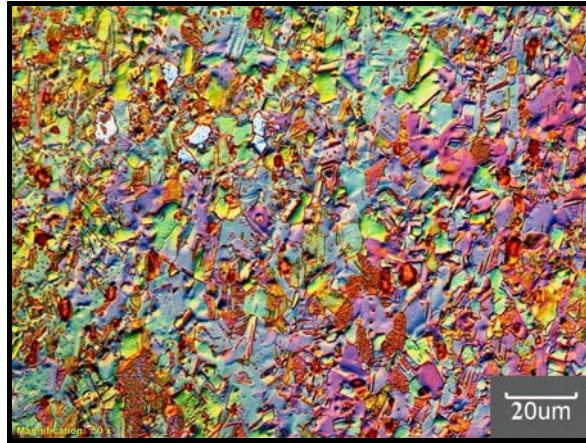


**Figure 1: Optical Micrograph of pure copper**



**Figure 2: I-STIR friction stir welding machine**

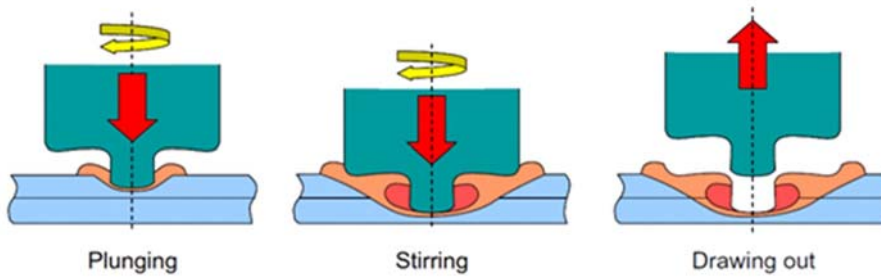


**Figure 3: A schematic illustration of the friction stir spot welding process**



Figure 4: Friction stir spot welded **sheet**

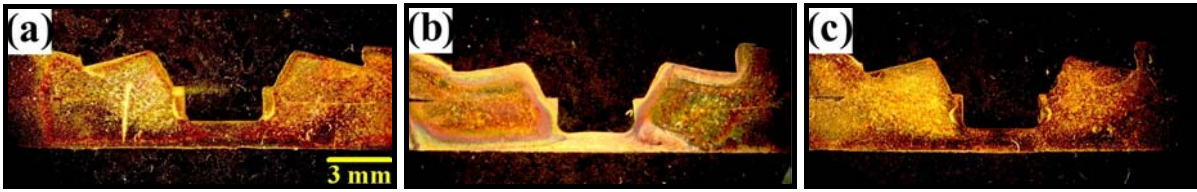


Figure 5: Macrograph of friction stir spot welded copper at; (a) 1200 rpm; (b) 1600 rpm and (c) 2000 rpm

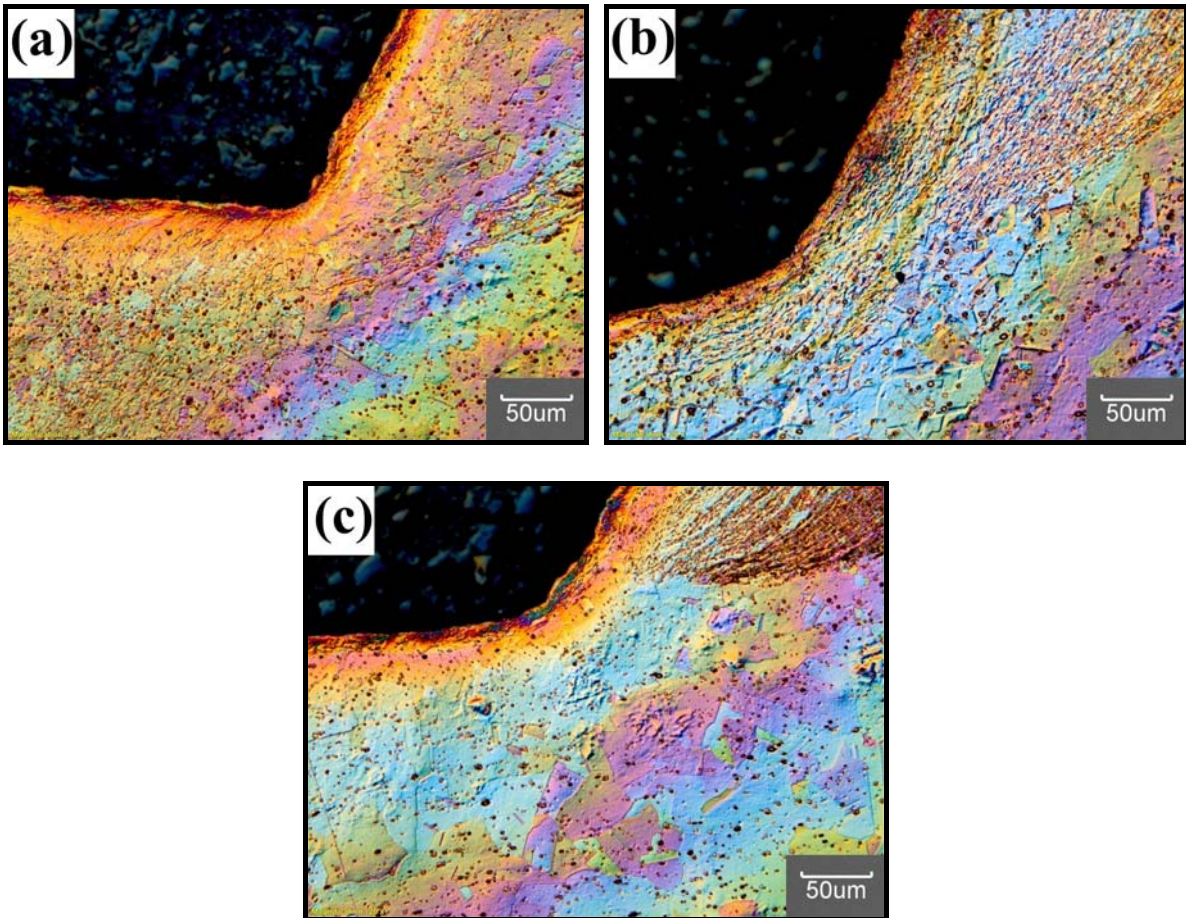
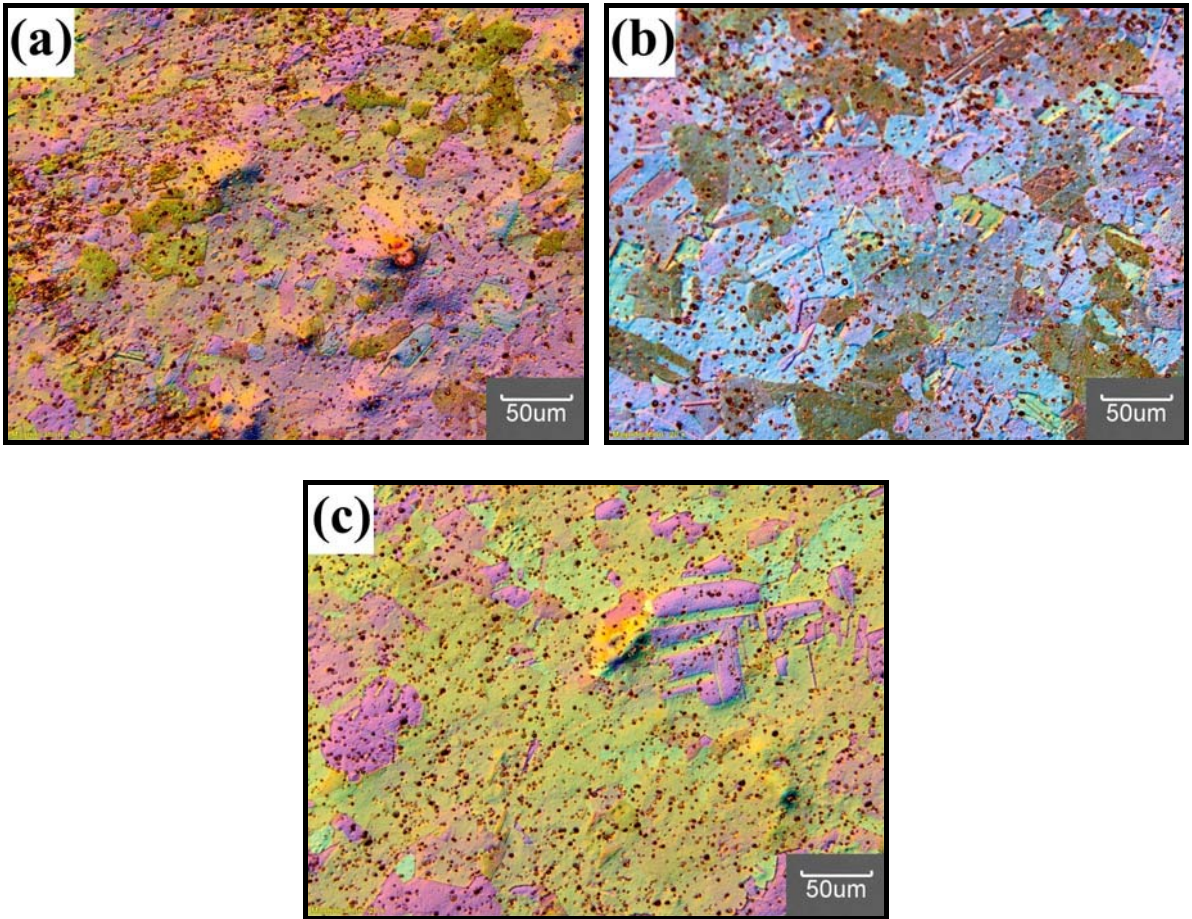
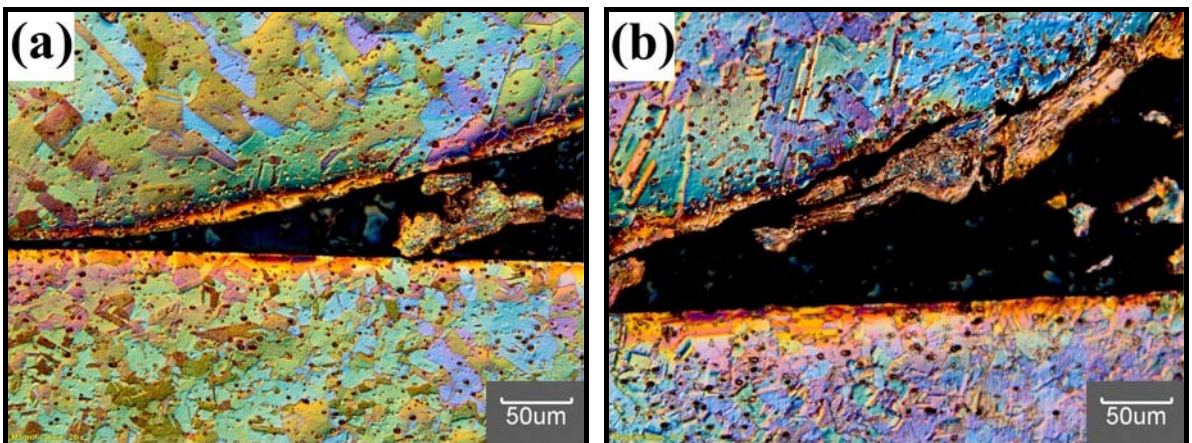
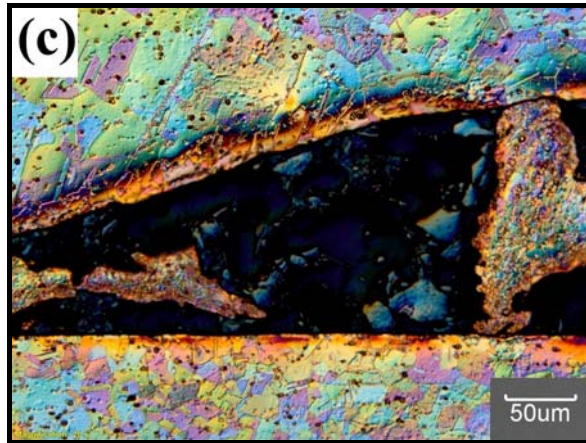


Figure 6: Optical Micrograph of transition zone of friction stir spot welded copper at; (a) 1200 rpm; (b) 1600 rpm and (c) 2000 rpm



**Figure 7: Optical Micrograph of heat affected zone of friction stir spot welded copper at; (a) 1200 rpm; (b) 1600 rpm and (c) 2000 rpm**





**Figure 8: Optical Micrograph of unbonded zone of friction stir spot welded copper at;**

**(a) 1200 rpm; (b) 1600 rpm and (c) 2000 rpm**

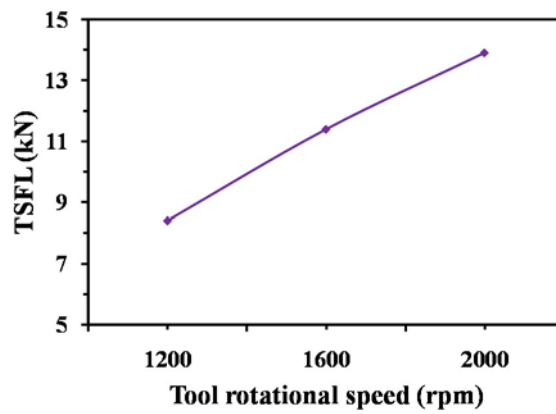


**Figure 9: Effect of tool rotational speed on tensile shear load of friction stir spot welded**

**copper**

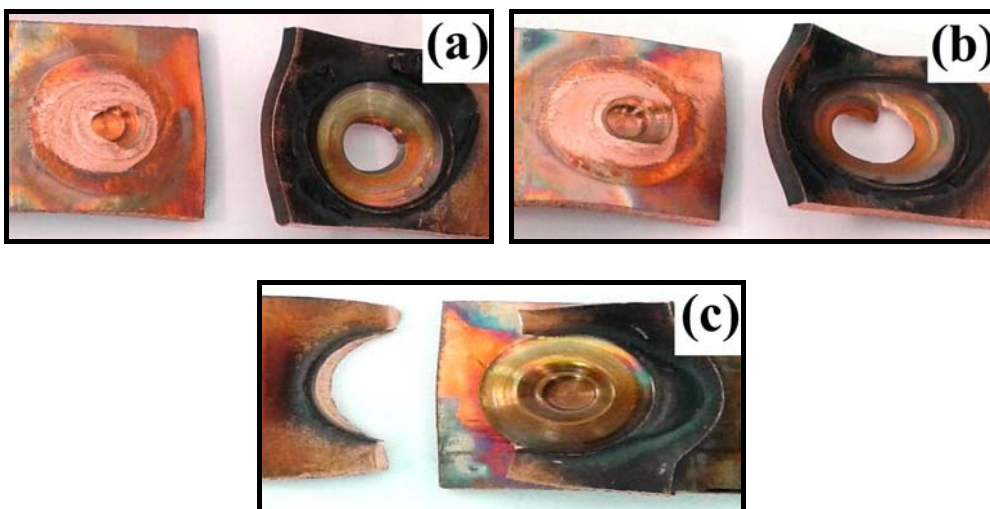


Figure 10: Photographs of failed sheets at tool rotational speed of; (a) 1200 rpm; (b) 1600 rpm and (c) 2000 rpm

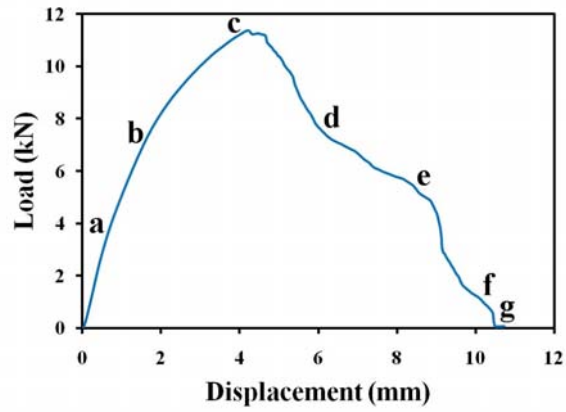
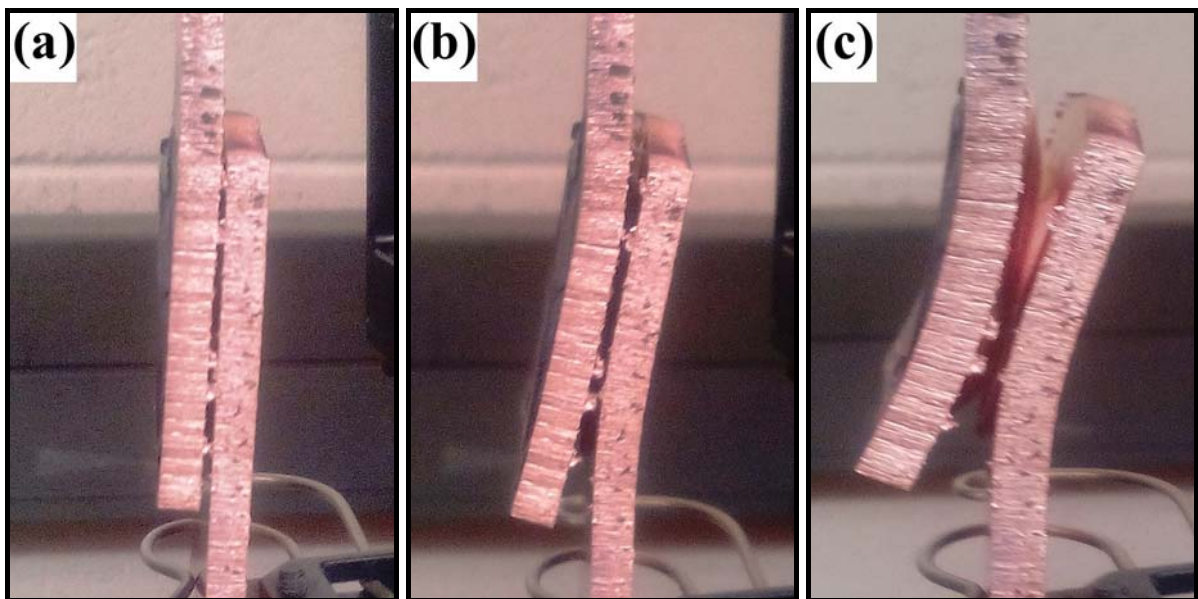
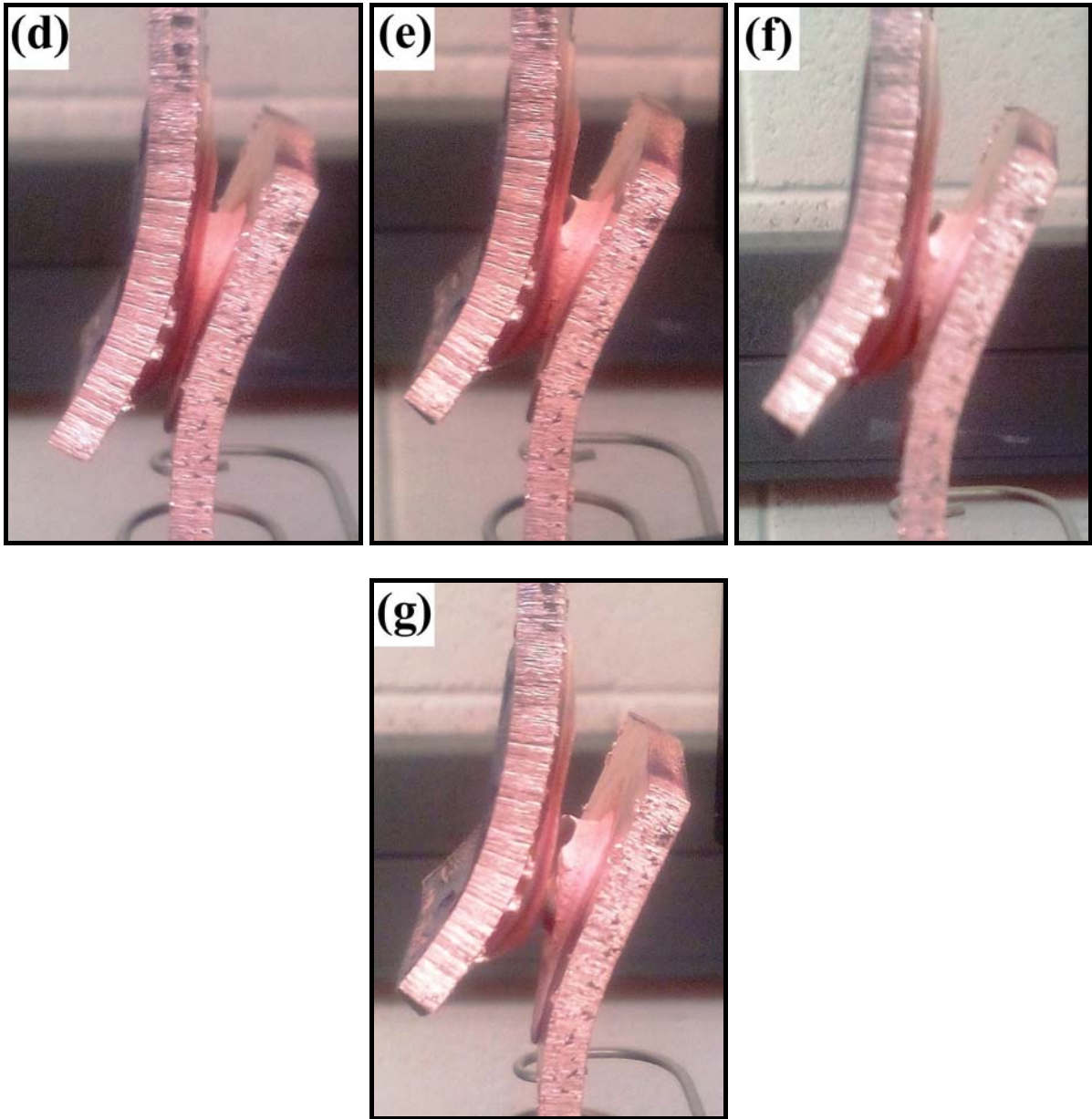


Figure 11: Load vs displacement graph of tensile shear tested specimen at tool rotational speed of 1600 rpm





**Figure 12: Photographs of tensile shear specimen during loading as marked in Figure**